

Contemporary Analytical Solutions in Terrestrial Photogrammetry

by

S. A. Veress
University of Washington
Department of Civil Engineering
Seattle, WA 98195
USA

ABSTRACT

Analytical terrestrial photogrammetry is used to monitor structural motions due to static or dynamic loading of the structure.

Three different analytical terrestrial photogrammetric systems are presented. The theory of each of these systems is discussed and accompanied with practical examples. These examples include monitoring of the Gabion Wall, monitoring the static and dynamic test of electric power lines and towers, and recording slide areas.

There are various forms of graphical evaluations which are presented. The economical feasibility of the methods and their practical applications are discussed.

1. Introduction

The general public recently became aware of the need for monitoring structures by the loss of human lives in various countries when large structures have failed.

There are numerous monitoring methods and instruments. Common characteristics of these methods and devices are that they provide one or seldom two dimensional information and that they must be installed during the construction. These internal monitoring methods must, therefore, be accompanied with an external monitoring system. The classical external monitoring system is considerably time consuming and point dependent, thus deformation can occur during the time of observation of the structure.

The public interest accompanied with technical problems led to the application of terrestrial photogrammetry for monitoring of structures. During this application, various types of analytical photogrammetric methods have been developed.

2. The Terrestrial Photogrammetric System

There are three systems presently practiced in the United States. One method is an analytical approach with fixed camera stations. The coordinates of the camera stations and the orientation angles are determined geodetically and considered constant. Then space intersection is computed to obtain the coordinates of the point of interest.

The method, using control points, is the most classical in that the control points are determined geodetically. They are considered as fixed and used to obtain the coordinates of camera stations and the orientation matrix of the photographs. The coordinates of points to be determined is obtained by space intersection.

The method, photogrammetric monitoring with combined measurements, is a simultaneous adjustment method. The camera orientation angles (ω , ϕ , κ) are determined by the phototheodolite. The base line is measured with an electronic distance measuring device. The coordinates of the frontal nodal

point of the camera are computed. These coordinates, as quasi observed quantities, are adjusted simultaneously with the orientation elements and the coordinates of the targets.

3. Analytical Approach with Fixed Camera Stations

This method is advantageous in the case of frequent monitoring for long periods of time. Special camera mounts should be built in order to insure that the camera will occupy the same position each time photographs are taken of the targets. The orientation angles of the camera and the coordinates of the camera stations are determined by ground measurements.

The photographic coordinates (x, y) are measured on a comparator. The mathematical model used for adjustment is the collinearity equation which is:

$$x_i - f \frac{m_{11} (X_o - X_0) + m_{12} (Y_o - Y_0) + m_{13} (Z_o - Z_0)}{m_{31} (X_o - X_0) + m_{32} (Y_o - Y_0) + m_{33} (Z_o - Z_0)} = x_i - F (X_o, Y_o, Z_o) \quad \dots\dots(3.1)$$

$$y_i - f \frac{m_{21} (X_o - X_0) + m_{22} (Y_o - Y_0) + m_{23} (Z_o - Z_0)}{m_{31} (X_o - X_0) + m_{32} (Y_o - Y_0) + m_{33} (Z_o - Z_0)} = y_i - F' (X_o, Y_o, Z_o)$$

The X_o, Y_o, Z_o are the precomputed approximate coordinates of the targets. The Taylor Series is used for linearization to obtain the observation equation for least-squares adjustment. These equations in a detailed form are:

$$\begin{matrix} v_{x_i} & = & \frac{\partial F}{\partial X_o} \Delta X & + & \frac{\partial F}{\partial Y_o} \Delta Y & + & \frac{\partial F}{\partial Z_o} \Delta Z & - & x_i & + & F(X_o, Y_o, Z_o) & \text{or } v & = & AX & - & L \\ \vdots & & \vdots & & \vdots & & \vdots & & \vdots & & \vdots & & & & & & \vdots & & \dots\dots\dots(3.2) \end{matrix}$$

The number of observation equations usually is six or eight because each point is photographed from three or four stations with convergent camera axes. From the least-squares adjustment the parameters and the standard errors are: $X = (A^T A)^{-1} A^T L, \quad \sigma_x = \sigma_o \sqrt{(A^T A)^{-1}}$

This method was used to monitor a Gabion Wall from 1975 to 1979. The Gabion Wall is part of the U. S. Interstate 90 freeway system and the project was sponsored by the Washington State Department of Transportation and the Federal Highway Administration.

Approximately 100 targets were mounted on the surface of the wall made of 3 mm thick aluminum painted white with a black dot at the center. The targets were photographed from a 1 km distance. A KA-2 camera with $f = 610$ mm was modified to take terrestrial photographs on a 23 x 23 cm, 6 mm thick glass negative. Kodak IV-F high contrast emulsion was used with the ASA rating of 50.

Three camera stations were anchored to the bedrock by reinforcement bars which were threaded on top to attach the camera mounts for each respective station.

The control net, which determined the coordinates of the camera stations (frontal nodal points) and the orientation angles of the photographs, were located on a 52 m wide existing road. The net was measured by a Kern DKM-3 theodolite and a DM 500 electronic distance measuring device. The standard error of the planimetric coordinates were found to be: σ_x or $y = \pm 1.7$ mm.

The elevation of the camera stations was determined by trigonometric leveling. The standard error of elevation is: $\sigma_z = \pm 4$ mm.

The photographic coordinates were obtained on a AP/C analytical plotter. The standard error of the photocoordinates were found to be ± 3.8 micrometers. The coordinates of the targets were computed for various photographs. The average standard error of the coordinates were found to be about ± 1.8 cm or better.

The first photographs were taken on September 7, 1976. The coordinates obtained from these photographs were considered to be "zero data" and each additional coordinate was compared to them. The differences in coordinates computed at each monitoring time were considered as deformations of the wall. A sample of this deformation is presented in Figure 1.

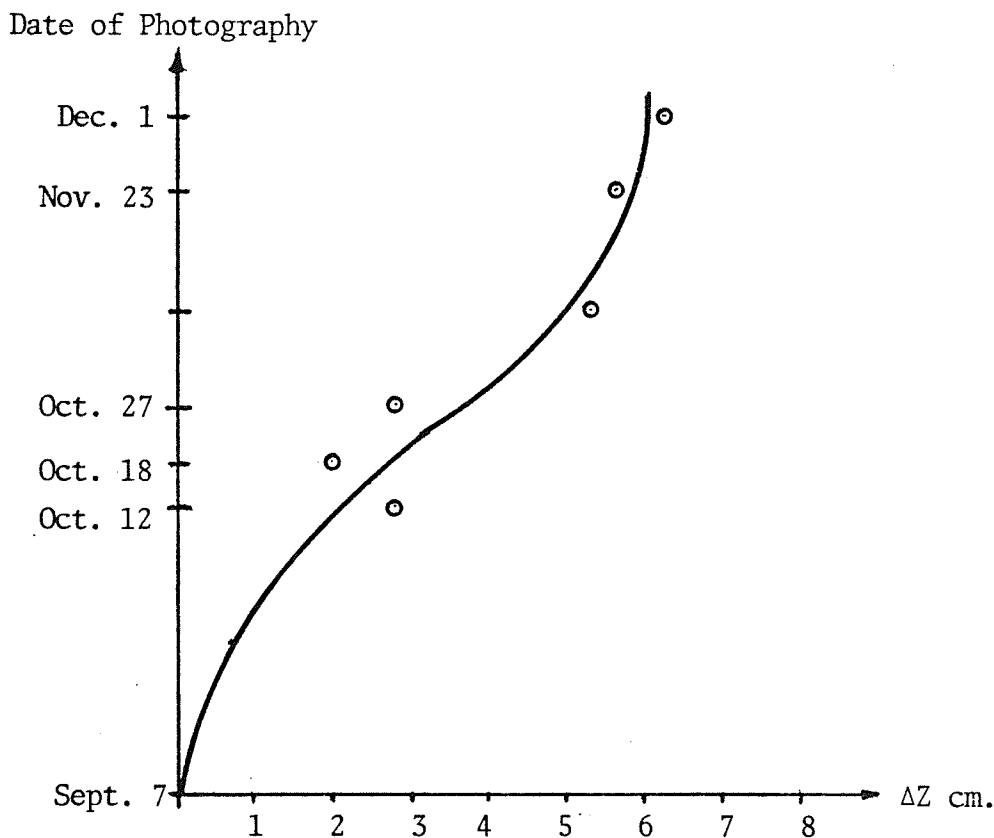


Figure 1. Deflection of a Point During Construction.

4. Terrestrial Photogrammetry Using Control Points

This method is one of the most popular; several projects are based on it. The camera used need not be a phototheodolite because the coordinates of the camera station and the orientation angles obtained from the control points were placed in the object space.

The mathematical model for this solution can be based on the collinearity equation (Eq. 3.1). If the camera has a narrow angle lens, which is usually the case in terrestrial photogrammetry, one may choose to write different mathematical models to achieve a higher degree of sensitivity.

The mathematical model for resection may be based on a comparison of the cosine of internal and external angles of rays. Figure 2. illustrates the geometrical principle.

Mathematically it can be formulated as:

$$\begin{aligned} \cos (aOb) - \cos (AOB) &= 0 \\ \cos (bOc) - \cos (BOC) &= 0 \\ \cos (aOc) - \cos (AOC) &= 0 \dots \dots \dots (4.1) \end{aligned}$$

where:

$$\cos (aOb) = \frac{x_a x_b + y_a y_b + f^2}{(aO) \cdot (bO)} \quad \text{similarly for } \cos (bOc)$$

The x_a, x_b, y_a, y_b , etc. are the photocordinates and f is the focal length. A similar expression cannot be written for the external angles because the station coordinates are not known. Only approximate values of these (X_o, Y_o, Z_o) can be used, thus the expression also becomes approximate.

Thus:

$$\cos (AOB)_o = \frac{(X_o - X_A)(X_o - X_B) + (Y_o - Y_B) + (Z_o - Z_A)(Z_o - Z_B)}{(AO) \cdot (BO)}$$

similarly for $\cos (BOC)$ and $\cos (AOC)$.

These expressions were substituted into formula (4.1) and after the application of the Taylor Series the observation equations can be formed.

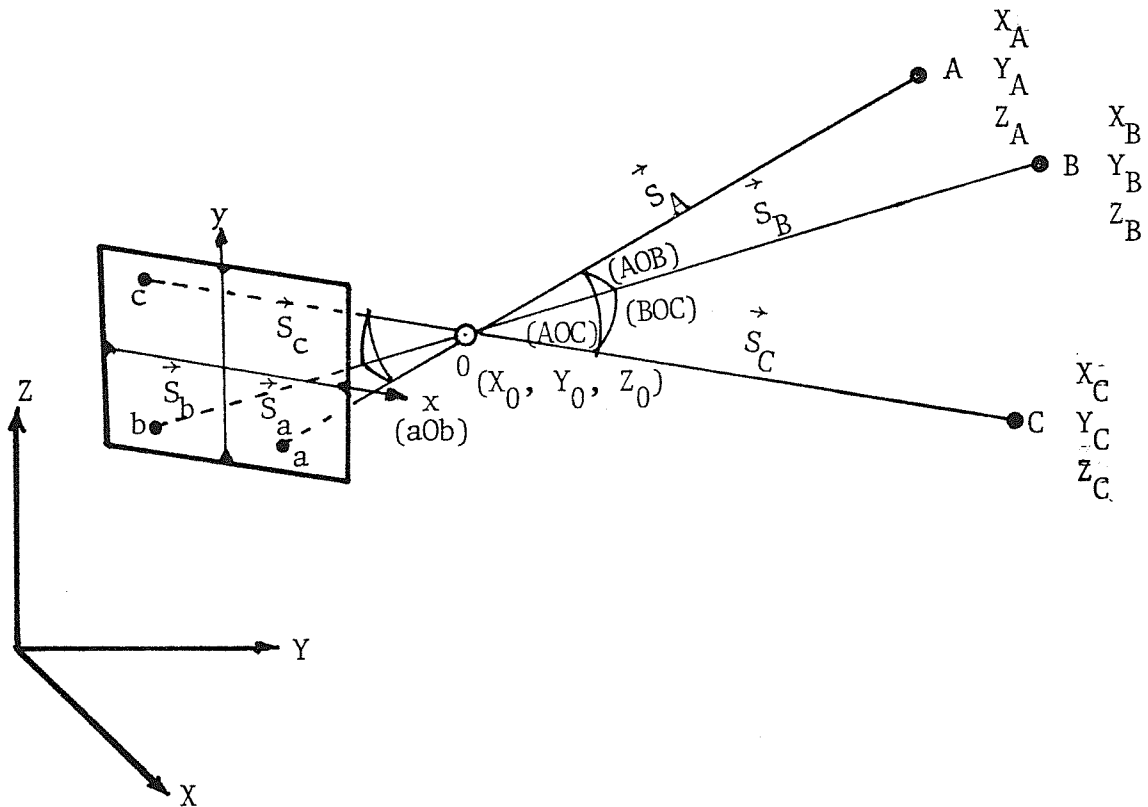


Figure 2. Geometrical Principle.

They are:

$$v_{ab} = \frac{\partial \cos(AOB)_0}{\partial X_0} \Delta X + \frac{\partial \cos(AOB)_0}{\partial Y_0} \Delta Y + \frac{\partial \cos(AOB)_0}{\partial Z_0} \Delta Z - [\cos(aOb) - \cos(AOB)_0] \dots \dots \dots (4.2)$$

where v is the correction. The least-squares adjustment was performed similarly to that shown by Eq. (3.1). The coordinates of the camera station are: $X = X_0 + \Delta X$, $Y = Y_0 + \Delta Y$, $Z = Z_0 + \Delta Z$.

These coordinates now serve as approximate coordinates for the next iteration. The iteration is carried out until $\Delta X = \Delta Y = \Delta Z = 0$.

The computation continues to obtain the orientation matrix (M) of the photographs. This process can be based on the comparison of vectors from the objective to the image and to the ground point. $\vec{S}_a, \vec{S}_b, \vec{S}_c$ and $\vec{S}_A, \vec{S}_B, \vec{S}_C$.

$$\begin{bmatrix} m_{11} & m_{12} & m_{13} \\ m_{21} & m_{22} & m_{23} \\ m_{31} & m_{32} & m_{33} \end{bmatrix} \begin{bmatrix} \cos xa0 \\ \cos ya0 \\ \cos za0 \end{bmatrix} = \begin{bmatrix} \cos XAO \\ \cos YAO \\ \cos ZAO \end{bmatrix} \dots \dots \dots (4.3)$$

The direction cosines for the picture and object space are computed from the corresponding unit vectors. Three vectors are required to arrive at a unique solution of the M matrix. Thus:

$$M = [\vec{S}_a \ \vec{S}_b \ \vec{S}_c]^{-1} [\vec{S}_A \ \vec{S}_B \ \vec{S}_C]$$

from this:

$$\begin{matrix} v_1 = \cos xa0 m_{11} + \cos ya0 m_{12} + \cos za0 m_{13} - \cos XAO \\ v_2 = \cos xb0 m_{11} + \cos yb0 m_{12} + \cos zb0 m_{13} - \cos YAO \\ \vdots \qquad \qquad \qquad \vdots \qquad \qquad \qquad \vdots \qquad \qquad \qquad \vdots \end{matrix} \quad \text{or } V = AX - L$$

The final step in the computation is the space intersection which was shown for the previous method by Eq. (3.2). There were several applications of the method during the last few years. One of the most significant is the measurement of structural behavior of the Moro 1200 KV test line for the U. S. Department of Energy, Bonneville Power Administration. A steel electric transmission tower has been tested by static and dynamic load. The deflections and deformations were monitored by photogrammetry.

The control points were determined from a quadrangle base net. All the angles and distances were measured by a Kern DK 500 electronic distance meter. The average standard errors of the coordinates were $\sigma_x = \pm 0.45$ mm $\sigma_y = \pm 0.65$ mm $\sigma_z = \pm 0.15$ mm. The control points were placed on and around the tower and they were coordinated from the base net.

The convergent photographs were taken with two MK 70 Hasselblads $f = 60$ mm. Nearly 700 photographs were taken and they were evaluated by the Bonneville Power Administration, Photogrammetric Section on a U. S. 1 Universal stereoplotter. Figure 3. shows such a photograph. The targets were located on both sides of the tower. The northern side targets, where the load was applied, were coded as the 300 series and the southern side was coded as the 200 series. The targets were made of 1/8 inch thick aluminium plates painted black on a white background.

Space resection was used to determine the camera positions as presented above. Then the orientation matrix was determined and space intersection was used to coordinate the targets. The average standard errors of the coordinates were $\sigma_x = \pm 3.2$ mm $\sigma_y = \pm 4.6$ mm $\sigma_z = \pm 3.9$ mm. This was confirmed by other methods

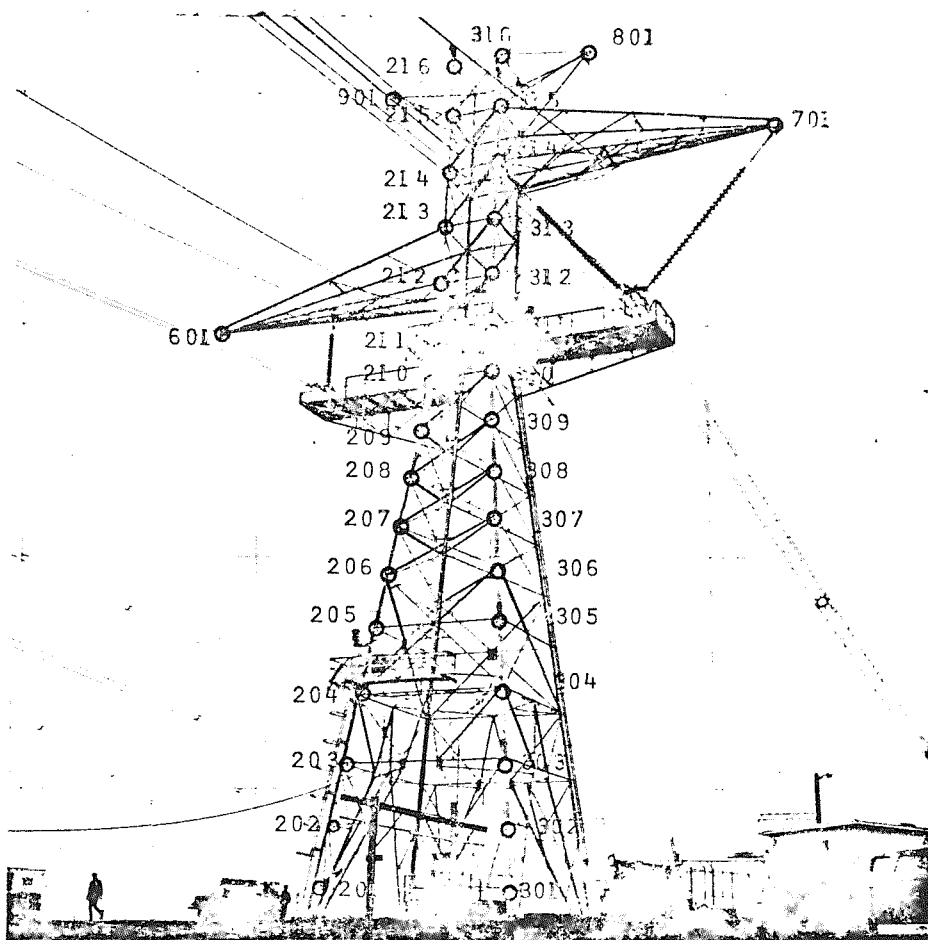


Figure 3. An MK 70 Photograph of the Test Tower.

The average standard error was computed between the photogrammetrically determined coordinates. The coordinates were obtained by a ground survey and were found to be approximately ± 5 mm.

The static tests were made by loading the tower up to 20,000 lbs. in 1,000 or 2,500 lbs. increments each of which were photographed. (The camera was not moved during the loading.) The loads that were applied were longitudinal, torsional, transverse and vertical pull.

Besides the tower, the conductor wires were also tested for static and dynamic load. The total of 563 negatives were utilized on which 29,447 points were measured on the U. S. 1 plotter; 18,648 coordinates were computed. The field control measurement required 112 man hours, 192 hours were needed for the measurements of the photographs and 136 hours were required to compute and plot the coordinates. The total of 440 productive hours were spent on the project. This shows the economical feasibility of the method.

Figure 4. shows a typical output of 9,000 lbs. transverse load (X axis is approximately in the direction of the wires). This form of data presentation is found to be very valuable. If one identifies the targets on Figure 3. and compares the 300 series, which was under load, to the 200 series, the individual deformation of the structural elements can be computed. For example; a twisting occurs at point 207 due to the load. The Bonneville Power Administration has used an harmonic computer plot where the amplitude of the dynamic motion in X, Y and Z direction was plotted as a function of time. From this data the damping coefficients were computed. The above example shows that the structural deformations associated with static or dynamic load can be obtained from photogrammetric monitoring. The stiffness values of the tower and the damping coefficient can then be determined.

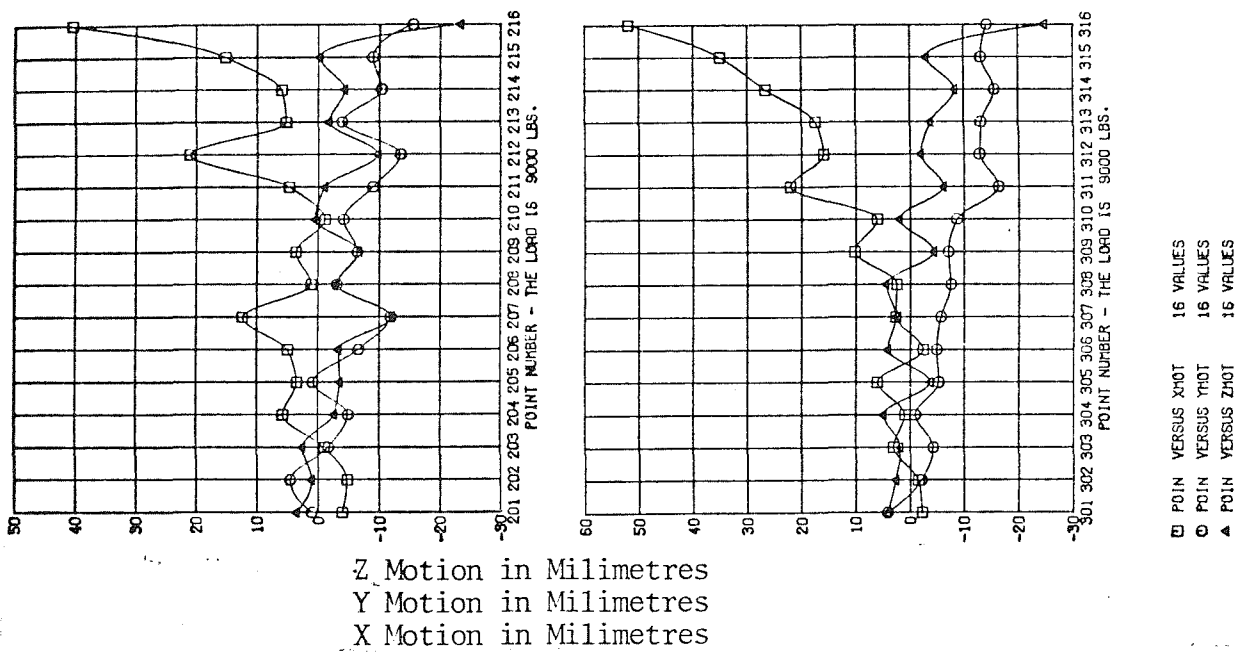


Figure 4. A Graphical Representation of Displacements.

5. Application of Combined Measurements

The combined analytical photogrammetric method tends to correct the economical and theoretical shortcomings of the previous methods. It was shown that the control survey may require as much as 25% of the total time needed to complete the project.

The combined photogrammetric method incorporates the field measurement by obtaining the orientation elements with a phototheodolite and a simultaneous adjustment of the geodetic and photogrammetric data. The direct measurement of the exterior orientation elements necessitates the use of a phototheodolite. The camera of the phototheodolite rotates around an axis passing through its gravity center to balance its weight. Thus, an eccentricity is introduced which must be determined before the computation is made.

The orientation matrix M is obtained from the measured orientation angles. Using the orientation matrix and the camera station coordinates the approximate coordinates (X_0, Y_0, Z_0) of the targets are obtained from Eq. (3.1) and (3.2) or from similar formulas. These measured and quasi measured quantities serve as an input into the final adjustments.

The final adjustments were based on collinearity equations; Eq. (3.1). In these equations all the measured quantities, the image coordinates, the elements of exterior orientation and the approximate coordinates of the targets, are considered as variables and are adjusted simultaneously. Linearization of these equations is required by the Taylor Series. If the corrections to the measured quantities are noted as v 's, then the most probable

values of the coordinates of the targets are as: $X = X_0 + \Delta X$, etc. Then the following equation is obtained:

$$\begin{aligned}
 v_{x_i} - \frac{\partial F}{\partial \omega} v_\omega - \frac{\partial F}{\partial \phi} v_\phi - \frac{\partial F}{\partial \kappa} v_\kappa + \frac{\partial F}{\partial X_0} v_X + \frac{\partial F}{\partial Y_0} v_Y + \frac{\partial F}{\partial Z_0} v_Z \\
 - \frac{\partial F}{\partial X_0} \Delta X - \frac{\partial F}{\partial Y_0} \Delta Y - \frac{\partial F}{\partial Z_0} \Delta Z + x_i - F(X_0, Y_0, Z_0) \\
 v_{y_i} - \frac{\partial F'}{\partial \omega} v_\omega - \frac{\partial F'}{\partial \phi} v_\phi - \frac{\partial F'}{\partial \kappa} v_\kappa + \frac{\partial F'}{\partial X_0} v_X + \frac{\partial F'}{\partial Y_0} v_Y + \frac{\partial F'}{\partial Z_0} v_Z \\
 - \frac{\partial F'}{\partial X_0} \Delta X - \frac{\partial F'}{\partial Y_0} \Delta Y - \frac{\partial F'}{\partial Z_0} \Delta Z + y_i - F'(X_0, Y_0, Z_0)
 \end{aligned}$$

or in a matrix form: $BV - AX + W = 0$(5.1)

Normal equations can be obtained from this combined observation and condition equations and the solution of the normal equation matrices are:

$$\begin{aligned}
 X &= -[A^T (B P^{-1} B^T)^{-1} A]^T A^T (B P^{-1} B^T)^{-1} W \dots \dots \dots (5.2) \\
 K &= -(B P^{-1} B^T)^{-1} (AX + W) \quad V^T PV = -K^T W
 \end{aligned}$$

the standard errors are computed as follows:

$$\sigma_o^2 = \frac{V^T PV}{r - u} \quad \sigma_x^2 = \sigma_o^2 [Q_{xx}] \quad Q_{xx} = [A^T (B P^{-1} B^T)^{-1} A]^T \dots \dots \dots (5.3)$$

where r and u are the number of conditions and unknowns respectively.

There were a number of practical projects conducted with this method. Here the Mud Mountain slide area project will be described as a representative. The project was initiated by the U. S. Corps of Engineers, Seattle District in October 1974 and is continuing. The slide area is photographed twice a year.

A modified Wild BC-4 Ballistic Camera with f 2.8 Astrotar lens, f-305 mm was used. The targets are styrofoam balls about 5 cm in diameter.

The photographs were made at a 520 m photographic distance and the average residual standard error of the coordinates of the target was found to be ± 9.1 mm.

The data representation was based on motion vectors and errors ellipses. Motion vectors were computed between two monitoring times by computing the distances between the two sets of coordinates of the same targets. The error ellipses in the XY plane were computed from the standard errors (Eq. 5.3). The motion vectors and the error ellipses are plotted and the elevations are written beside the point. Such a plot is shown by Figure 5. where the error ellipses are regarded as the inherent errors of the system. The slide area, as shown, has been active from 1974 to 1977 and stabilized after that.

6. Discussion

The practical application of these methods indicates that the most economical method is monitoring with fixed camera stations, if long range monitoring is required. The fabrication of the camera mount can be done well for long focal length cameras. The spatial repeatability to occupy the same position for each monitoring time is about ± 40 micrometers.

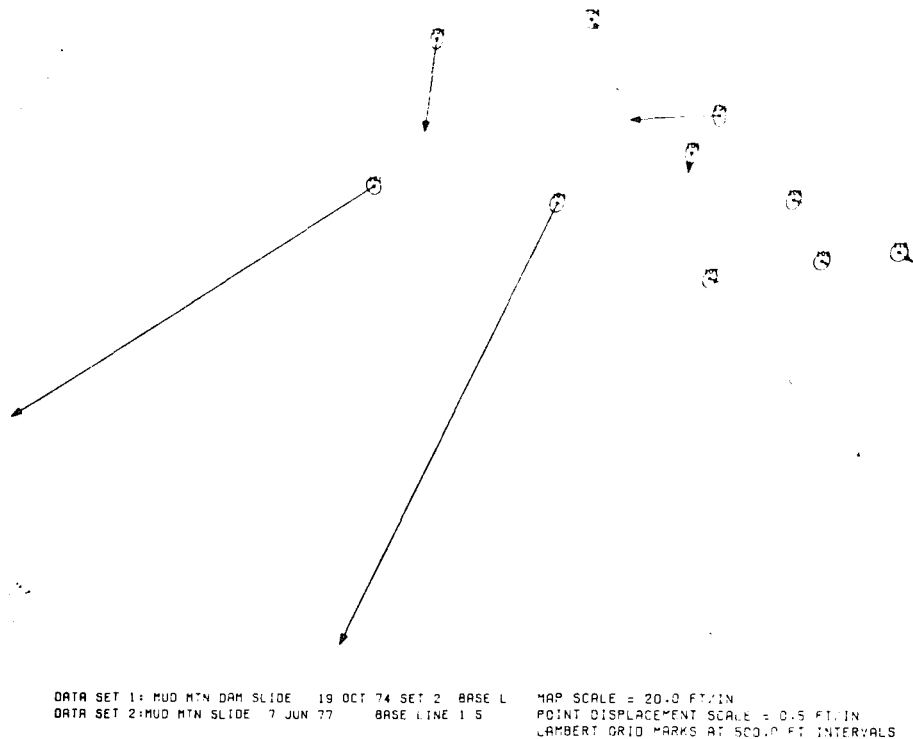


Figure 5. Error Ellipses and Motion Vectors.

The method, utilizing control points, has a wide range of application, but not without limitations. The basic problem is under certain conditions it is very difficult to place four control points in such a location that would provide a strong geometry for the space resection. If the control points are located too closely to each other, the determination of the rotational elements particularly ω , become uncertain. This is because the lower portion of the photographs are usually occupied by technically useless foreground, whereas the upper portion is the sky. This is shown by the following formula:

$$\sigma_{\omega} = \sqrt{\frac{7f^2}{18a^4}}$$

where f is the focal length of the camera and a is the distance of the control point from x axis of the photograph. It was found, by experimentation, that if $2a < 1/3$ is the format size the determination of the ω rotation is not sufficiently accurate for a precise analytical photogrammetry project.

Monitoring with combined measurement is capable of providing a high accuracy with a good economy. The economical advantage is obtained by direct measurements of the exterior orientation elements. It is unfortunate, however, that there are very few phototheodolites on the market capable of providing these measurements with a desired 1-0.1 of a second of arc least reading. This fact requires a practitioner to modify an instrument to obtain the needed data economically. Nevertheless, it can be recognized that the application of terrestrial photogrammetry with analytical solutions is increasing and more frequent use is expected in the future.

Acknowledgement

The author would like to express his gratitude to Mr. J. P. Erlandson, Chief of the Surveying Branch of the U. S. Corps of Engineers, Seattle District. To Dr. J. N. Hatzopoulos, the University of Washington and Mr. W. C.

Wilson, Chief of the Photogrammetric Branch of the Bonneville Power Administration for their valuable contributions.

Selected References

1. Brandenberger, A. J. and Erez, M. T., "Photogrammetric Determination of Deformations in Large Engineering Structures," Canadian Surveyor, Vol. 26, No. 2, 1972.
2. Cotovanu, E., "Messung von Brucken durch terrestrische Photogrammetrie," Buletin de Fotogrammetrie, Special Issue, 1972.
3. Erlandson, J. P., Peterson, J. C. and Veress, S. A., "The Modification and Use of the BC-4 Camera for Measurements of Structural Deformations," Proceedings of A.S.P., Sept., 1974.
4. Erlandson, J. P. and Veress, S. A., "Contemporary Problems in Terrestrial Photogrammetry," Photogrammetric Engineering, Vol. XL, pp. 1079-1085, 1974.
5. Erlandson, J. P. and Veress, S. A., "Monitoring Deformations of Structures," Photogrammetric Engineering and Remote Sensing, Vol. 41, No. 11, 1975.
6. Erlandson, J. P. and Veress, S. A., "Photogrammetrische Erfassung von Bauwerksveranderungen," VR-Vermessungswesen und Raumordnung, Vol. 8, 1976.
7. Gutu, A., "Photogrammetric Measurement Accuracy of Wall Pillar Cracks in Rock Salt Mines," Buletin de Fotogrammetric, Special Issue, 1972.
8. Veress, S. A., "Adjustment by Least-Squares," American Congress on Surveying and Mapping, 1974.
9. Veress, S. A., "Determination of Motion and Deflection of Retaining Walls," Part I and II, University of Washington, Final Technical Report, 1971.
10. American Society of Photogrammetry, "Handbook of Non-Topographic Photogrammetry," 1979.